

Active and Reactive Power Control Strategy for Grid-Connected Six-Phase Generator by using Multi-Modular Matrix Converters

David CABALLERO*, Federico GAVILAN*, Edgar MAQUEDA*,
Raúl GREGOR*, Jorge RODAS*, Derlis GREGOR†

*Laboratory of Power and Control Systems, †Laboratory of Distributed Systems
Facultad de Ingeniería, Universidad Nacional de Asunción

Luque, CP 2060, Paraguay

E-mail: {dcaballero, fgavilan, emaqueda, rgregor, jrodas & dgregor}@ing.una.py

and

Sergio TOLEDO††, Marco RIVERA††

††Faculty of Engineering, Universidad de Talca

Talca, CP 747 - 721, Chile

E-mail: {stoledo & marcoriv}@utalca.cl

ABSTRACT

This paper proposes an active and reactive power control strategy based on predictive control approaches applied to grid-connected renewable energy systems. To accomplish this a multi-modular matrix converter topologies are used in combination with a simple but efficient grid synchronization strategy. The theoretical performance analysis is performed considering a six-phase wind energy generator system interconnected with the grid. Results based on a MATLAB/Simulink simulation environment are discussed and the most relevant characteristics of the proposed control technique are highlighted considering the total harmonic distortion and the mean squared error as a parameters of performance.

Keywords: Predictive control, matrix converters, renewable energy systems, multiphase induction generator.

1. INTRODUCCION

In the last years the interest in power generation from renewable energy sources has experienced a significant growth, mainly justified by the reduced environmental impact generated. Renewable energy systems (RES), such as solar photovoltaic (PV), micro-hydraulic and wind energy systems are widely used as an alternative to the traditional systems. A very active research area in the field of RES are focused in the multiphase wind energy generator (MWEG) systems [1], [2]. In particular, MWEG systems with multiple three-phase windings are very convenient for wind turbine (WT) applications, due to important aspects especially for high-power safety-critical applications such as performance, reliability, smooth torque and partition of power [3]. In MWEG, the six-phase wind energy generator (SpWEG) with two sets of three-phase stator windings spatially shifted by 30 electrical degrees and isolated neutral points is probably one of the most widely discussed topology with fully rated back-to-back converter system to grid-connected applications [4]-[6]. Consequently with the development of multiphase topologies and drives, recent research efforts have

been focused in the development of a flexible power interface based on a modular architecture capable to interconnecting different renewable energy sources and load, including energy storage systems to the electrical grid. These efforts converge in the multi-modular matrix converter (MMC) topologies whose the main feature is the ability to provide a three-phase sinusoidal voltages with variable amplitude and frequency using fully controlled bi-directional electronic switches without the use of energy storage elements [7]. These characteristics makes plausible the use of MMC in applications where are required high power density and compact converters such as SpWEG systems, constituting an attractive alternative if it is compared with conventional converter topologies [8], [9].

The main contribution of this paper comparing with the previous works will focus on a theoretical performance analysis of a MMC combined with a SpWEG scheme in order to ensure an efficient active and reactive power control from the generator side to the grid side. Each module of the MMC architecture are connected in cascade to the independent three-phase windings of the SpWEG. A model-based predictive control (MPC) technique is used to predict the effects of future control actions in order to minimize a defined cost function. The control criterion will be the active and reactive power control.

This paper is organized as follows: Section 2 describes the mathematical model of the MMC. Section 3 presents a detailed description of the MPC control strategy. Section 4 discusses the simulation results and a performance analysis of the proposed predictive control technique using the total harmonic distortion (THD) and the mean square error (MSE) as a parameters of performance. Finally, the main remarks are summarized in Section 5.

2. POWER CONVERSION MODEL

The proposed topology consists of two three-phase matrix converter (MC) modules connected to the SpWEG by using a passive (LC) input filter and then connected to the grid by an output filter, as it was shown in Fig. 1. Each one of

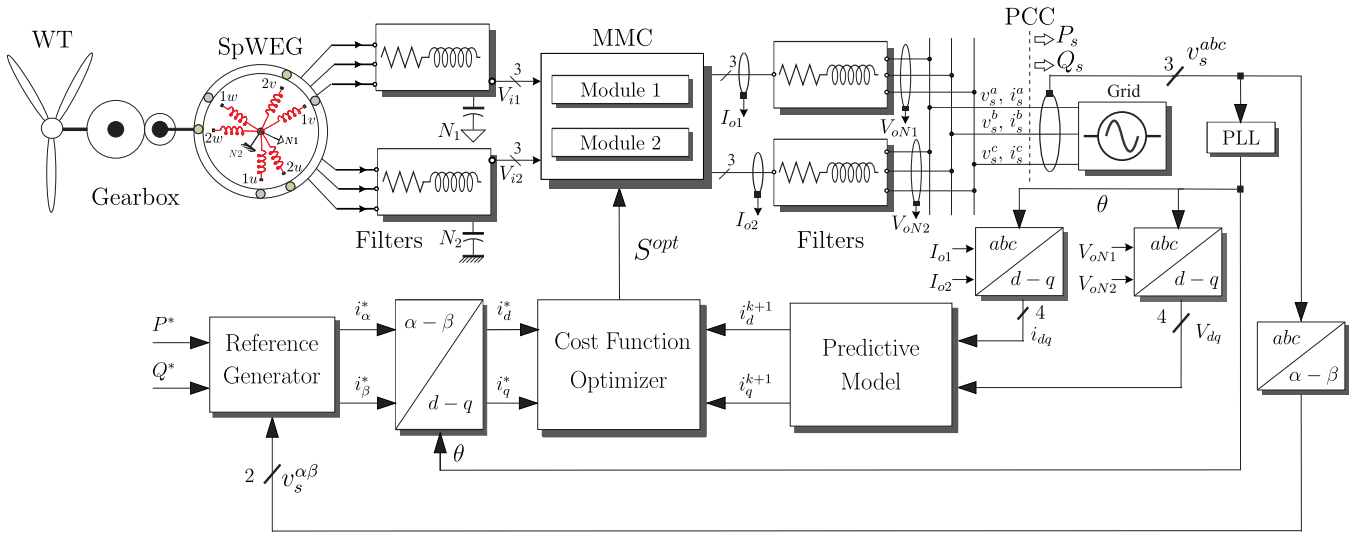


Fig. 1. Proposed multi-modular matrix converter and power control topology applied to the six-phase wind energy generator.

these modules is represented by the power electronic scheme of Fig. 2. In this case, generated voltages by the SpWEG are indicated as V_{uj} , V_{vj} and V_{wj} where $j \in \{1, 2\}$ depending of the corresponding module. In the same way, the generated currents are indicated as I_{uj} , I_{vj} and I_{wj} . The output currents of the input filter are indicated as I_{eu} , I_{ev} and I_{ew} , respectively. Input voltages of the MC are V_{euj} , V_{evj} and V_{ewj} . The output voltages of the MC respect to the corresponding SpWEG neutral point (N_1 or N_2) are V_{aNj} , V_{bNj} and V_{cNj} . Moreover, output currents are I_{oaj} , I_{obj} and I_{ocj} , respectively. Finally, the output filter voltages (that are connected to the grid) are V_{oaNj} , V_{obNj} and V_{ocNj} .

The MC power topology is composed of nine bi-directional power switches, which can generate 27 switching states [10]. If the three-phase vectors of voltages and currents are defined as:

$$V_{sj} = \begin{bmatrix} V_{uj} \\ V_{vj} \\ V_{wj} \end{bmatrix} \quad V_{ij} = \begin{bmatrix} V_{euj} \\ V_{evj} \\ V_{ewj} \end{bmatrix} \quad V_{oj} = \begin{bmatrix} V_{aNj} \\ V_{bNj} \\ V_{cNj} \end{bmatrix} \quad (1)$$

$$I_{sj} = \begin{bmatrix} I_{uj} \\ I_{vj} \\ I_{wj} \end{bmatrix} \quad I_{ij} = \begin{bmatrix} I_{euj} \\ I_{evj} \\ I_{ewj} \end{bmatrix} \quad I_{oj} = \begin{bmatrix} I_{oaj} \\ I_{obj} \\ I_{ocj} \end{bmatrix} \quad (2)$$

then the following vectorial equations relate the input and output voltages or currents in terms of the switching states of the MC:

$$V_{oj} = S \cdot V_{ij}, \quad I_{ij} = S^T \cdot I_{oj} \quad (3)$$

being S the instantaneous transfer matrix, defined as:

$$S = \begin{bmatrix} S_{ua} & S_{ub} & S_{uc} \\ S_{va} & S_{vb} & S_{vc} \\ S_{wa} & S_{wb} & S_{wc} \end{bmatrix} \quad (4)$$

where the S_{xy} element has a binary value, corresponding to the state of the single switch.

In order to avoid short circuits on the input side and ensure an uninterrupted current flow on the load side, the switching signals

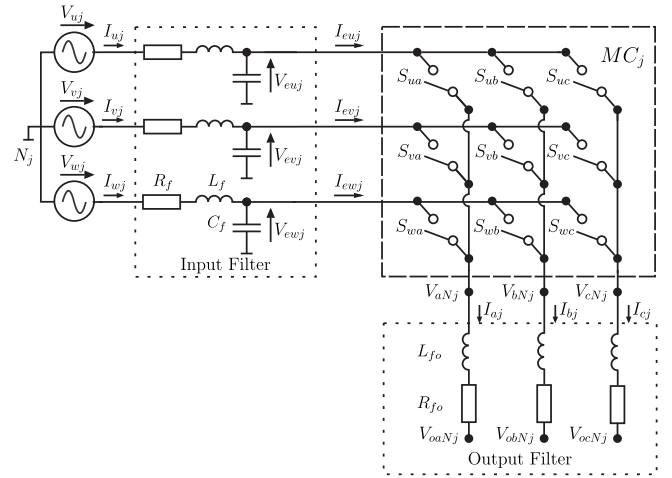


Fig. 2. Model of the power systems.

S_{xy} must satisfy the following condition:

$$S_{uy} + S_{vy} + S_{wy} = 1 \quad y \in \{a, b, c\}. \quad (5)$$

The dynamic model of the passive output filter is defined as:

$$V_{oj} - V_{oNj} = L_{fo} \frac{dI_{oj}}{dt} + R_{fo} I_{oj} \quad (6)$$

where:

$$V_{oNj} = \begin{bmatrix} V_{oaNj} \\ V_{obNj} \\ V_{ocNj} \end{bmatrix} \quad (7)$$

is the voltage vector measured from the end of the output filter to the corresponding neutral point N_j of the SpWEG.

In the case of the input filter, the dynamic behavior can be directly modeled by using the space-state representation approach as:

$$\frac{d}{dt} \begin{bmatrix} V_{ij} \\ I_{sj} \end{bmatrix} = A_c \begin{bmatrix} V_{ij} \\ I_{sj} \end{bmatrix} + B_c \begin{bmatrix} V_{sj} \\ I_{ij} \end{bmatrix} \quad (8)$$

where:

$$A_c = \begin{bmatrix} 0 & \frac{1}{C_f} \\ -\frac{1}{L_f} & -\frac{R_f}{L_f} \end{bmatrix} \quad B_c = \begin{bmatrix} 0 & -\frac{1}{C_f} \\ \frac{1}{L_f} & 0 \end{bmatrix} \quad (9)$$

being L_f and C_f the filter inductance and capacitance, respectively, and R_f is the leakage resistance of L_f .

3. PROPOSED CONTROL METHOD

A. Predictive model

The MPC technique uses a model of the real system to predict the future behavior of the variables to be controlled. The inherent discrete nature of power converters simplifies the MPC optimization algorithm to the prediction of the system behavior only for the set of feasible switching states. This approach is known as finite control set MPC, and it has been successfully used in several power converter applications and topologies [11].

The discrete model of the system using the forward Euler discretization is defined as follows [12]:

$$I_{oj}(k+1) = \left(1 - \frac{R_{fo}T_m}{L_{fo}}\right) I_{oj}(k) + \frac{T_m}{L_{fo}} (V_{oj}(k) - V_{oNj}(k)) \quad (10)$$

where T_m is the sampling time, $I_{oj}(k)$ and $V_{oNj}(k)$ are measured, and $V_{oj}(k)$ is calculated for all switch combinations to predict the next value of the output currents and evaluate the cost function in order to select the optimum solution.

B. References generation

Active and reactive power references in currents terms are defined by the following equations [13]:

$$i_{\alpha}^* = \frac{2}{3} \frac{v_{s\alpha}}{v_{s\alpha}^2 + v_{s\beta}^2} P_s^* + \frac{2}{3} \frac{v_{s\beta}}{v_{s\alpha}^2 + v_{s\beta}^2} Q_s^* \quad (11)$$

and

$$i_{\beta}^* = \frac{2}{3} \frac{v_{s\beta}}{v_{s\alpha}^2 + v_{s\beta}^2} P_s^* - \frac{2}{3} \frac{v_{s\alpha}}{v_{s\alpha}^2 + v_{s\beta}^2} Q_s^* \quad (12)$$

where P_s^* and Q_s^* denote the active and reactive power references, respectively, while $v_{s\alpha}$ and $v_{s\beta}$ are the grid voltages in stationary reference frame $(\alpha - \beta)$.

C. Cost function

The cost function can be defined as a deviation between the references and predicted currents and is normally defined as follows:

$$J = \| e_{id}(k+1) \|^2 + \| e_{iq}(k+1) \|^2 \quad (13)$$

where

$$\| e_{id}(k+1) \| = \| i_d^*(k+1) - i_d^p(k+1) \|$$

$$\| e_{iq}(k+1) \| = \| i_q^*(k+1) - i_q^p(k+1) \|$$

$\| \cdot \|$ denotes vector magnitude, and $i_{dq}^*(k+1)$ and $i_{dq}^p(k+1)$ are vectors which contain the reference and prediction currents, respectively in the dynamic reference frame $(d - q)$. The predictions are based on the current states and control efforts.

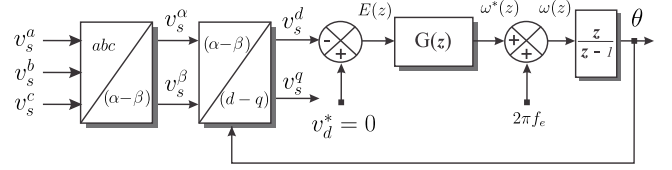


Fig. 3. Block diagram of a PLL with special design of the compensator.

D. Digital PLL implementation

The dynamic performance of the proposed PLL is highly influenced by the compensator $G(z)$, Fig. 3 shows the proposed PLL diagram block. Considering that the reference signal is the grid voltage in d axis, and since the loop gain includes an integral term, θ must track the constant component of the reference signal with zero steady-state error. However, to ensure zero steady-state error, the loop gain must include at least two integrators. Therefore, $G(z)$ must include at least one integral term, that is, one pole at $z = 1$. The other poles and zeros of $G(z)$ are determined mainly by the closed-loop bandwidth requirements of the PLL and stability indices such as phase margin and gain margin, according with the procedure described in [14]. Due to the fact that $G(z)$ is controllable, the transfer function can be expressed into controllable canonical form as follows:

$$\mathbf{x}(k+1) = [\mathbf{F}]_{5 \times 5} [\mathbf{x}(k)]_{5 \times 1} + [\mathbf{D}]_{5 \times 1} [e(k)]_{5 \times 1} \quad (14)$$

$$\omega^*(k) = [\mathbf{C}]_{1 \times 5} [\mathbf{x}(k)]_{5 \times 1} \quad (15)$$

where the matrix $[\mathbf{F}]_{5 \times 5}$; and the vectors $[\mathbf{D}]_{5 \times 1}$, and $[\mathbf{C}]_{1 \times 5}$ define the dynamics of the PLL compensator $[G(z)]$. The set of state variables are defined as follows:

$$[\mathbf{F}]_{5 \times 5} = \begin{bmatrix} 2.5 & -2.2 & 0.9 & -0.2 & 0.01 \\ 1 & 0 & 0 & 0 & 0 \\ 0 & 1 & 0 & 0 & 0 \\ 0 & 0 & 1 & 0 & 0 \\ 0 & 0 & 0 & 1 & 0 \end{bmatrix} \quad (16)$$

$$[\mathbf{D}]_{5 \times 1} = [1 \ 0 \ 0 \ 0 \ 0]^T \quad (17)$$

$$[\mathbf{C}]_{1 \times 5} = [1.7 \ -5.7 \ 8.1 \ -5.8 \ 1.6]. \quad (18)$$

This state-space realization is called controllable canonical form because the resulting model is guaranteed to be controllable.

E. Optimizer

The optimization process is performed by evaluating the cost function for each valid switching state. The search space given by the set of possible vectors can be defined as $\varepsilon = \phi_i^{\phi_o}$, where ϕ_i and ϕ_o are the number of the matrix converter input and output phases, respectively. For the particular case of a three-phase grid-connected system, the search space is defined by 27 possible vectors for performing the control law. The optimization algorithm selects the optimum vector S^{opt} which minimizes the cost function J , as detailed in Algorithm 1.

Algorithm 1 Optimization algorithm

1. Initialize $J_o^1 := \infty, J_o^2 := \infty$
 2. Compute MMC input voltages (Eqn. 2)
 3. **while** $i \leq \varepsilon$ **do**
 4. Compute MMC output voltages (Eqn. 3)
 5. Compute the prediction of the states (Eqn. 10)
 6. Compute the cost function (Eqn. 13)
 7. **if** $J_1 < J_o^1$ **then**
 8. $J_o^1 \leftarrow J_1, S_1^{opt} \leftarrow S_i$
 9. **end if**
 10. **if** $J_2 < J_o^2$ **then**
 11. $J_o^2 \leftarrow J_2, S_2^{opt} \leftarrow S_i$
 12. **end if**
 13. $i = i + 1$
 14. **end while**
 15. Apply the optimum vector $S^{opt} \in \{S_1^{opt}, S_2^{opt}\}$
-

4. SIMULATION RESULTS

The MMC has been modeled in MATLAB/Simulink in order to validate the proposed control scheme, considering the electrical parameters that are shown in Table I. Simulations have been performed to show the accuracy of the MPC technique. Numerical integration by means of the first order Euler algorithm has been applied to obtain the evolution of the controlled variables. Fig. 4 shows the accuracy of the proposed method and the voltage and current behavior at the point of common coupling (PCC). Fig. 4 (upper) shows the instantaneous active power reference change. The active power reference was initially set to 4,000 W and after $t = 0.06$ s, the value of the power reference was changed to 2,000 W. It can be seen that the output power follows its reference value, similar results are obtained at $t = 0.12$ s and $t = 0.18$ s. On the other hand, Fig. 4 (middle), shows the tracking current dynamic performance for a step of the active power reference. As can be seen the dynamic response during the transient is very fast and the steady-state error is near to zero. Finally, Fig. 4 (bottom) shows the current and voltage behavior in the PCC. When the reference power decreases, the current amplitude decreases, keeping constant the voltage value.

To evaluate the proposed control performance the THD, Eqn. (19), and the MSE, Eqn. (20), are used as a figures of merit.

TABLE I
ELECTRICAL PARAMETERS

PARAMETER	SpWEG MPC Power Control		
	SYMBOL	VALUE	UNIT
Electrical signal frequency	f_s	50	Hz
Grid voltage signal amplitude	V_s	380	V
Input filter resistance	R_f	0.5	Ω
Input filter inductance	L_f	0.4	mH
Input filter capacitance	C_f	25	μ F
Output filter resistance	R_{fo}	4.7	Ω
Output filter inductance	L_{fo}	3	mH
Switching period	T_m	20	μ s
Active power reference	P^*	4,000	W
Reactive power reference	Q^*	0	VAR

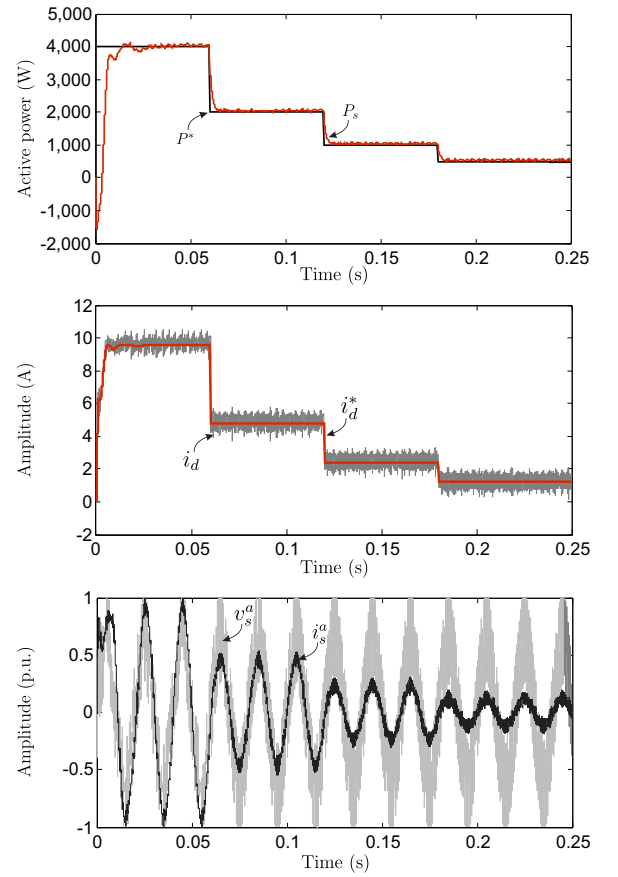


Fig. 4. Performance analysis: (upper) active power evolution, (middle) tracking current in dynamic reference frame and (bottom) PCC voltage and current behavior.

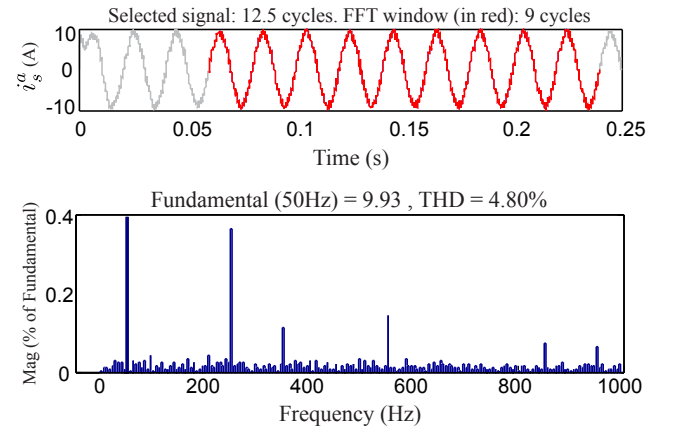


Fig. 5. Performance analysis: (upper) grid current, (bottom) grid current THD.

$$THD = \sqrt{\frac{1}{i_1^2} \sum_{i=2}^N i_i^2} \quad (19)$$

$$MSE(\Psi) = \sqrt{\frac{1}{N} \sum_{j=1}^N \Psi_j^2} \quad (20)$$

where N is the number of vector elements, i_1 is the amplitude of the fundamental frequency of the analyzed current, i_i are the current harmonics and Ψ represents the difference between the measured value and reference value of the analyzed signal. In Fig. 4 (middle) it can be also appreciated that the currents fluctuate slightly due to the switching electronic components of the MMC, generating a small harmonic distortion. For an active power of $P^* = 4,000$ W and a switching period of $20 \mu\text{s}$. It can be seen that the THD is always below 5 %. Similar results are obtained for B and C phases. MSE was quantified on steady state, between the reference and measurement currents in ($d-q$) reference frame, and the obtained value is 0.0952.

5. CONCLUSION

In this paper an active and reactive power control strategy based on the predictive control approaches applied to grid-connected SpWEG systems has been proposed. To achieve the instantaneous power control, a MMC architecture has been used in combination with the predictive control. The simulation results confirm the capability of the proposed predictive control technique mainly in terms of low harmonic distortion, and also showing an acceptable dynamic response when a multi-step power references is applied. Finally, the proposed control technique has proved to be viable providing an unity power factor allowing independently active power control.

Acknowledgment

The authors would like to thank the Paraguayan Government for their encouragement and kind financial support provided through the CONACYT grant project (14-INV-097) and the Linking Program of Scientists and Technologists (PVCT16-187). This work was also funded by FONDECYT Regular Project No. 1160690. In addition, they wish to express their gratitude to the anonymous reviewers for their helpful comments and suggestions.

6. REFERENCES

- [1] J. Rodas, H. Guzman, R. Gregor, and F. Barrero, "Model predictive current controller using Kalman filter for fault-tolerant five-phase wind energy conversion systems," in **Proc. 7th PEDG**, Vancouver, Canada, 2016, pp. 1–6.
- [2] J. Rodas, Gregor, Y. Takase, D. Gregor, and D. Franco, "Multi-modular matrix converter topology applied to the six-phase wind energy generator," in **Proc. 50th UPEC**, Stoke-on-Trent, U.K., 2015, pp. 1–6.
- [3] M. J. Duran and F. Barrero, "Recent advances in the design, modeling, and control of multiphase machines: Part II," **IEEE Transactions on Industrial Electronics**, Vol. 63, No. 1, pp. 459–468, 2016.
- [4] P. Maciejewski and G. Iwanski, "Modeling of six-phase double fed induction machine for autonomous dc voltage generation," in **Proc. 10th EVER**, Monte-Carlo, Monaco, 2015, pp. 1–6.
- [5] N. Rathika, A. Senthil Kumar, P. Sivakumar, and S. Rahul, "Analysis and control of multiphase synchronous generator for renewable energy generation," in **Proc. ICAEE**, Vellore, India, 2014, pp. 1–6.
- [6] A. S. Kumar and T. Cermak, "A novel method of voltage regulation of isolated six-phase self-excited induction generator fed vsi driven by wind turbine," in **Proc. ICSOEB**, Sousse, Tunisia, 2015, pp. 1–6.
- [7] M. Lopez, J. Rodriguez, C. Silva, and M. Rivera, "Predictive torque control of a multidrive system fed by a dual indirect matrix converter," **IEEE Transactions on Industrial Electronics**, Vol. 62, No. 5, pp. 2731–2741, 2015.
- [8] C. Garcia, M. Rivera, M. Lopez, J. Rodriguez, R. Pena, P. Wheeler, and J. Espinoza, "A simple current control strategy for a four-leg indirect matrix converter," **IEEE Transactions on Power Electronics**, Vol. 30, No. 4, pp. 2275–2287, 2015.
- [9] S. Toledo, M. Rivera, R. Gregor, J. Rodas, and L. Comparatore, "Predictive current control with reactive power minimization in six-phase wind energy generator using multi-modular direct matrix converter," in **Proc. 8th ANDESCON**, Arequipa, Peru, 2016, pp. 1–4.
- [10] M. Vijayagopal, P. Zanchetta, L. Empringham, L. D. Lillo, L. Tarisciotti, and P. Wheeler, "Modulated model predictive current control for direct matrix converter with fixed switching frequency," in **Proc. EPE-ECCE Europe**, Geneva, Switzerland, 2015, pp. 1–10.
- [11] S. Vazquez, J. Rodriguez, M. Rivera, L. G. Franquelo, and M. Norambuena, "Model predictive control for power converters and drives: Advances and trends," **IEEE Transactions on Industrial Electronics**, Vol. 64, No. 2, pp. 935–947, 2017.
- [12] S. Toledo, R. Gregor, M. Rivera, J. Rodas, D. Caballero, F. Gavilán, and E. Maqueda, "Multi-modular matrix converter topology applied to distributed generation systems," in **Proc. 8th IET PEMD**, Glasgow, U.K., 2016, pp. 1–6.
- [13] P. Anu, R. Divya, and M. Nair, "STATCOM based controller for a three phase system feeding single phase loads," in **Proc. TAP Energy**, Kollam, India, 2015, pp. 333–338.
- [14] S. Golestan and J. M. Guerrero, "Conventional synchronous reference frame phase-locked loop is an adaptive complex filter," **IEEE Transactions on Industrial Electronics**, Vol. 62, No. 3, pp. 1679–1682, 2015.